

A controllability-based formulation for the topology optimization of smart structures

Juliano F. Gonçalves^{*1}, Jun S.O. Fonseca^{1a} and Otávio A.A. Silveira^{2b}

¹Department of Mechanical Engineering, Federal University of Rio Grande do Sul, R: Sarmiento Leite 425, CEP 90050-170, Porto Alegre, Brazil

²Department of Civil Engineering, Federal University of Santa Catarina, R: João Pio Duarte da Silva 205, CEP 88040-970, Florianópolis, Brazil

(Received April 21, 2015, Revised February 11, 2016, Accepted February 16, 2016)

Abstract. This work presents a methodology to distribute piezoelectric material for structural vibration active control. The objective is to design controlled structures with actuators which maximizes the system controllability. A topology optimization was formulated in order to distribute two material phases in the domain: a passive linear elastic material and an active linear piezoelectric material. The objective is the maximization of the smallest eigenvalue of the system controllability Gramian. Analytical sensitivities for the finite element model are derived for the objective functions and constraints. Results and comparisons with previous works are presented for the vibration control of a two-dimensional short beam.

Keywords: piezoelectric actuators; controllability Gramian; topology optimization

1. Introduction

Vibration control has been subject of much research lately due to the increasing use of smart structures in several engineering applications. Piezoelectric ceramics are extensively used as the active part of smart materials, both for sensors and actuators (Kumar and Narayanan 2008, Gupta *et al.* 2011). Thus, there is a need for methodologies to place the active material within structures as sensors and actuators. Measures able to quantify the control effectiveness can be used to choose this optimal placement. The controllability of a linear system can be determined by evaluating the controllability Gramian. Thereby, the control actuators performance can be qualitatively predicted: the system is considered controllable if this Gramian is non-singular (Gawronski 2004). However, this concept is a pass/no-pass test and is not particularly useful for the problem of optimal location of actuators.

Several authors have proposed performance indices based on optimal control theory. Hamdan and Nayfeh (1989) focused the problem of modal controllability measures using generalized angles between the eigenvectors of the system matrix and columns of the input matrix. This

*Corresponding author, M.Sc., E-mail: juliano.fagundes@ufrgs.br

^a Ph.D., E-mail: jun@ufrgs.br

^b D.Sc., E-mail: otavio.silveira@ufsc.br

measure was extended considering the physical significance of each mode and its respective degrees of controllability (Kim and Junkins 1991). An energy-based quantitative measure for controllability and observability was proposed by Hać and Liu (1993); a performance index was defined taking into account the total energy, which is highly dependent on the low-order modes, and a term proportional to the energy contribution of each mode. For systems with small damping coefficients and well-spaced natural frequencies, expected energies for each mode are related to the Gramian eigenvalues. Gawronski and Kim (1996) used Hankel singular value (HSV) to quantify the degree of controllability and observability for a set of sensors and actuators (S/A). For lightly damped structures, the singular values of individual S/A pairs can be used to approximate a more complex system.

A pioneering work of simultaneous optimization of structure and control system was developed by Onoda and Haftka (1987) where a combined cost is minimized subject to a constraint on the magnitude of the response to a given disturbance which involves both the rigid-body and elastic modes. Ou and Kikuchi (1996) studied the optimal design of a controlled structure by means of the homogenization method and the displacement feedback law. Topology optimization for the design of piezoelectric transducers was treated by Silva and Kikuchi (1999). This formulation was based on a definition of the electromechanical coupling coefficient, which provides the piezoelectric effectiveness on the conversion of mechanical into electrical energy, or the converse. Different objective functions were defined aiming to maximize the response of a specific operating mode, to design the transducer with a specific resonance frequency or to a particular frequency bandwidth.

Wang and Wang (2001) worked on the controllability of actuators in beam structures. This paper presented a quantitative index, obtained through a singular value decomposition (SVD) of the input matrix. This index provides information on the actuator energy to be supplied to the structure and can be used to determine the optimal location of piezoelectric actuators. The problem of vibration control using piezoelectric actuators can be extended to more complex structures, such as shell structures (Sohn *et al.* 2011).

Some recent works have studied the design of piezoelectric devices by means of the topology optimization method. Takezawa *et al.* (2010) developed a structural topology optimization formulation for single- and multi-axis load cell structures using the SIMP and the projection methods. Ruiz *et al.* (2013), optimized the distribution of passive material and the polarization profile of bonded piezoelectric material layer, in order to maximize the sensor output for a static loading. The topology optimization of piezoelectric actuator/sensor attached to a thin-shell structure was studied by Zhang and Kang (2014) in order to improve the active control performance for reducing the dynamic response under transient excitations employing a constant gain velocity feedback control algorithm. Takezawa *et al.* (2014a) carried out the optimization of vibration energy harvester, and specifically, the poling direction of the material in order to avoid cancellations due to different electric potential signals. This formulation aims to maximize the electromechanical coupling coefficient. Since these devices are usually designed with piezoelectric material between electrodes, electric field cancellation can occur. The optimization of piezoelectric transducer layout for energy-recycling semi-active vibration control system was studied by Takezawa *et al.* (2014b) considering space structure composed of trusses. The objective function was defined as the integration of the square of all displacement over the whole analysis time domain. Silveira *et al.* (2015), proposed a smart structure topology design methodology using piezoelectric material to control structural vibration. For that, two material phases were considered: a passive elastic isotropic material and a piezoelectric material which composes the active fraction (actuators). Topology optimization was used to select either passive or active material in each

point of the structure maximizing the controllability Gramian trace for an LQR control system.

In this work, the optimization methodology to distribute piezoelectric material for structural vibration active control (Silveira *et al.* 2015) is improved considering a new controllability measure. Although the latter work has obtained successful designs, a large trace does not necessarily imply a non-singular Gramian which is required for a system to be completely state controllable. By adopting the maximization of the smallest eigenvalue of the Gramian instead of its trace, the system controllability can be assured. A sequential linear programming (SLP) is used to solve the topology optimization problem. After this, the controller synthesis is performed and its performance is compared regarding the controllability measure used as objective function.

2. Coupled finite element model

The smart structure is considered a three-dimensional body composed by linear elastic and linear piezoelectric materials. The parameterization that defines the elastic properties (\mathbf{C}), piezoelectric coupling properties (\mathbf{E}), dielectric properties ($\boldsymbol{\varepsilon}$) and density (γ) of the interpolated material is given by

$$\mathbf{C} = \rho^\alpha \mathbf{C}_{pzt} + (1 - \rho^\alpha) \mathbf{C}_{elas} \quad (1)$$

$$\mathbf{E} = \rho^\beta \mathbf{E}_{pzt} \quad (2)$$

$$\boldsymbol{\varepsilon} = \rho^\delta \boldsymbol{\varepsilon}_{pzt} \quad (3)$$

$$\gamma = \rho \gamma_{pzt} + (1 - \rho) \gamma_{elas} \quad (4)$$

where ρ is the design variable (more details in section 4), \mathbf{C}_{elas} and \mathbf{C}_{pzt} are the elastic properties of non piezoelectric and piezoelectric material respectively; \mathbf{E}_{pzt} and $\boldsymbol{\varepsilon}_{pzt}$ define the electromechanical coupling and dielectric properties of the piezoelectric material; γ_{elas} and γ_{pzt} are the density for each material. The convergence stability of the optimization process depends on the penalty exponents α , β and δ . Intrinsic and objective-dependent conditions for this problem were proposed by Kim *et al.* (2010). However, since we are interested in the discrete design the penalty exponent values used in this work followed Silveira *et al.* (2015) in order to validate the numerical implementation and compare their solutions. Thus, elastic isotropic material is obtained when $\rho=0$ and piezoelectric material is obtained when $\rho=1$.

A continuum finite element model formulation (Allik and Hughes 1995) for infinitesimal strains is used. The global finite element model that governs the spatial movement and balance of electrical charges is given by

$$\mathbf{M}_{uu} \ddot{\mathbf{u}} + \mathbf{C}_{uu} \dot{\mathbf{u}} + \mathbf{K}_{uu} \mathbf{u} = -\mathbf{K}_{u\phi} \boldsymbol{\phi} + \mathbf{f} \quad (5)$$

$$\mathbf{K}_{u\phi}^T \mathbf{u} + \mathbf{K}_{\phi\phi} \boldsymbol{\phi} = \mathbf{q} \quad (6)$$

where \mathbf{u} and $\boldsymbol{\phi}$ are, respectively, the vectors for mechanical and electrical degrees of freedom, \mathbf{M}_{uu} is the global mass matrix, \mathbf{C}_{uu} is the global damping matrix, \mathbf{K}_{uu} is the global stiffness matrix, $\mathbf{K}_{u\phi}$ is the global piezoelectric coupling matrix, and $\mathbf{K}_{\phi\phi}$ is the global dielectric capacitance matrix.

These matrices depend on the design variables ρ . Moreover, in Eqs. (5) and (6), \mathbf{f} is the vector of external mechanical forces and \mathbf{q} is the vector of electric charges. The electrical degrees of freedom are defined as the actuator known electrical inputs. Therefore, the term regarding the piezoelectric coupling was considered as an external force.

In this work, the state-space representation is defined in modal coordinates. Therefore, the order of the system can be reduced, which is desirable when complex structures are modeled and analyzed by a finite element method. A truncated modal matrix can be used in the transformation from the nodal coordinates to modal coordinates. Since the poles of the reduced model are a subset of the poles of the full model, a reduced model of a truncated stable model always produces a stable reduced model (Gawronski 2004). Thereby, the displacement vector can be approximated by the superposition of the m most representative modes

$$\mathbf{u} \approx \Psi \boldsymbol{\eta} = \sum_{i=1}^m \Psi_i \eta_i \quad (7)$$

where Ψ is the truncated modal matrix and $\boldsymbol{\eta}$ is the corresponding vector of modal coordinates.

Assuming a structural viscous damping model to the flexible structure

$$\mathbf{C}_{uu} = 2\mathbf{Z}\mathbf{K}_{uu}^{1/2}\mathbf{M}_{uu}^{1/2} \quad (8)$$

and substituting Eq. (7) in (5), the truncated damped modal finite element model of the structure with piezoelectric actuators can be written as

$$\boldsymbol{\eta} + 2\mathbf{Z}\boldsymbol{\Omega}\boldsymbol{\eta} + \boldsymbol{\Omega}^2\boldsymbol{\eta} = -\Psi^T\mathbf{K}_{u\phi}\boldsymbol{\phi} + \Psi^T\mathbf{f} \quad (9)$$

where $\boldsymbol{\Omega}$ and \mathbf{Z} are $m \times m$ diagonal matrices of natural frequencies and modal damping respectively.

An important advantage of this type of model is its definition of damping properties. The damping matrix is usually not known, however is conveniently evaluated in the modal coordinates. More details concerning structural models in nodal and modal coordinates can be found in Gawronski (2004).

3. Active control of structures

3.1 State-space representation

A linear time-invariant system of finite dimensions is described by the following system of constant coefficient linear differential equations (Gawronski 2004)

$$\dot{\mathbf{x}} = \mathbf{A}\mathbf{x} + \mathbf{B}\mathbf{u}^c \quad (10)$$

$$\mathbf{y} = \mathbf{D}\mathbf{x} \quad (11)$$

where the N -dimensional vector \mathbf{x} is the state vector, the s -dimensional vector \mathbf{u}^c is the system input, and the r -dimensional vector \mathbf{y} is the system output; \mathbf{A} , \mathbf{B} , and \mathbf{D} are the system, input and

output matrices, respectively.

The state-space representation carries information about the internal structure of the model, which is represented by the states. A state contains the minimal number of physical variables that allows calculating uniquely the output using the applied input (Gawronski 2004). Assuming the truncated modal displacements and velocities as state variables, the vector of state variables can be written as

$$\mathbf{x} = \{\boldsymbol{\eta} \quad \dot{\boldsymbol{\eta}}\}^T \quad (12)$$

Dealing with free vibrations, the open-loop system represented in Eq. (10) can be fully determined through the electrical input vector $\mathbf{u}^c = \boldsymbol{\varphi}$, and the system and electrical input matrices, given by

$$\mathbf{A} = \begin{bmatrix} \mathbf{0} & \mathbf{I} \\ -\boldsymbol{\Omega}^2 & -2\mathbf{Z}\boldsymbol{\Omega} \end{bmatrix} \quad \mathbf{B} = \begin{bmatrix} \mathbf{0} \\ -\boldsymbol{\Psi}^T \mathbf{K}_{u\varphi} \end{bmatrix} \quad (13)$$

where all terms were previously defined.

3.2 Linear quadratic regulator theory

An effective way to design a feedback control system is using the optimal linear quadratic regulator (LQR), which is the simplest and the most frequently used formulation. Considering the system presented in Eq. (10), a linear state feedback is evaluated with a constant gain which minimizes a quadratic cost functional (Burl 1999, Preumont 2002)

$$J = \frac{1}{2} \int_0^{t_f} (\mathbf{x}^T \mathbf{Q} \mathbf{x} + \mathbf{u}^{cT} \mathbf{R} \mathbf{u}^c) dt \quad (14)$$

where \mathbf{Q} is a positive semi-definite weighting matrix for the state variables and \mathbf{R} is a positive definite weighting matrix for the control inputs.

Following Silveira *et al.* (2015), this work considers the LQR control theory in steady state, then the feedback gain matrix is given by $\mathbf{G} = \mathbf{R}^{-1} \mathbf{B}^T \mathbf{P}$, where the matrix \mathbf{P} is the solution of the algebraic Riccati equation

$$\mathbf{A}^T \mathbf{P} + \mathbf{P} \mathbf{A} - \mathbf{P} \mathbf{B} \mathbf{R}^{-1} \mathbf{B}^T \mathbf{P} + \mathbf{Q} = \mathbf{0} \quad (15)$$

Considering free vibrations of the smart structure, the closed-loop state-space equation can be written as

$$\dot{\mathbf{x}} = (\mathbf{A} - \mathbf{B} \mathbf{G}) \mathbf{x} \quad (16)$$

In this work, the number of states used for control and for observation are the same and depends on the analyzed case. Furthermore, these states are assumed to be completely observable and can be directly related to the outputs.

A feedback control system based on a truncated model is not necessarily stable for the residual modes, which may cause unforeseen effects in the observation and control (spillover). These

problems can degrade the system performance to the uselessness point amplifying disturbances outside the bandwidth (Vasques and Rodrigues 2006). Methods to reduce the spillover effect are discussed by a number of authors (Balas 1978, Meirovitch 1990). However, this issue is not in the scope of this work, which considers all states known at any given time.

3.3 Controllability of a structural modal model

In control theory, controllability measures the ability of a particular set of actuators to control all the states of a system. For an asymptotically stable system, i.e., if all poles (eigenvalues) of \mathbf{A} have negative real part, the system response is limited and the covariance matrix for steady state is bounded (Preumont 2002). Thus, the system response to a group of independent white noise of unit intensity is given by

$$\mathbf{W}_c = \int_0^{\infty} e^{\mathbf{A}\tau} \mathbf{B}\mathbf{B}^T e^{\mathbf{A}^T\tau} d\tau \quad (17)$$

which is called controllability Gramian. For a general time-invariant system, as Eq. (10), one can obtain the controllability Gramian, more conveniently, from the Lyapunov equation (Gawronski 2004)

$$\mathbf{A}\mathbf{W}_c + \mathbf{W}_c\mathbf{A}^T + \mathbf{B}\mathbf{B}^T = \mathbf{0} \quad (18)$$

As in Eq. (15), the Gramian evaluation requires the solution of a Lyapunov equation which can be obtained through a well known algorithm (Bartels and Stewart 1972). The system is controllable if all states can be excited by the control input. This condition is fully satisfied if and only if \mathbf{W}_c is positive definite (Preumont 2002).

4. Topology optimization

Topology optimization aims to distribute materials within a given fixed design domain V , for a given set of loads S , and boundary condition S_u , as shown in Fig. 1. This distribution is determined by the minimization of an objective function.

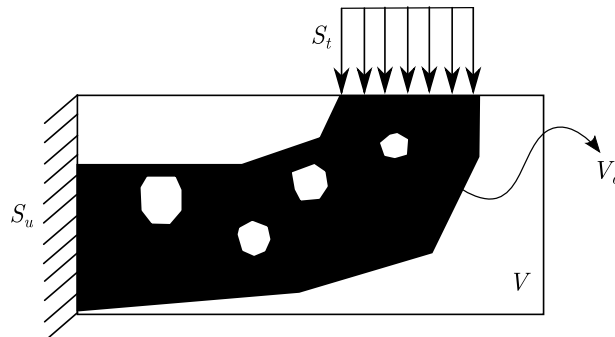


Fig. 1 Topology optimization design

The solution for a topology optimization, such as the one represented in Fig. 1, consists in subdomains V_d each one filled with one of the materials. The optimal material distribution is influenced by the given volume fraction constraints. Since the design domain is discretized into n_e finite elements, the usual choice is to assume element-wise constant fraction. The design variables are defined in each finite element, where ρ_i is the pseudo-density for the i -th element. The discrete value (0 or 1) of ρ_i describes which material fills the respective finite element, according to the material interpolation.

The integer optimization of the continuous problem is ill posed, and its spatial discretization might not converge with the mesh refinement. Therefore, it can be formulated a relaxed continuous optimization which introduce a constitutive parameterization that allows the design variables to assume intermediate values (Bendsøe 1989, Bendsøe and Kikuchi 1988). In order to enable the interpretation of the optimal distribution of material, it is desirable that the structure presents almost entirely piezoelectric or elastic isotropic material. Therefore, intermediate values of the design variable ρ_i are penalized in order to be forced toward either 0 or 1 (Bendsøe and Kikuchi 1988, Bendsøe and Sigmund 1999, Sigmund and Petersson 1998).

4.1 Proposed optimization formulation

In most applications, a structure may be submitted to two types of disturbance: transient or persistent. Considering a transient disturbance, the control aims to return from the disturbed state to a desired state in a given time, using the minimum control effort. This condition is achieved by placing the set of actuators in a configuration where some norm of the controllability Gramian is maximized. For the latter case, the set of actuators must minimize the persistent disturbance, i.e., the energy transmitted to the structure from the actuators should be as large as possible. However, considering systems with small damping coefficients and well-spaced natural frequencies, either criteria can be employed for the actuator placement problem regardless the type of disturbance (Hać and Liu 1993, Leleu *et al.* 2001).

The controllability Gramian \mathbf{W}_c for a general set of parameters in state-space (\mathbf{A} , \mathbf{B}) is obtained by solving the Lyapunov equation presented in Eq. (19) (Gawronski 2004). The eigenvalues for this Gramian can be obtained through

$$(\mathbf{W}_c - \lambda_j \mathbf{I}) \boldsymbol{\sigma}_j = \mathbf{0} \tag{19}$$

$$\boldsymbol{\sigma}_j^T \boldsymbol{\sigma}_j = 1 \quad j = 1, 2, \dots, m \tag{20}$$

where \mathbf{I} is the identity matrix, λ_j is the j -th eigenvalue of \mathbf{W}_c , and $\boldsymbol{\sigma}_j$ is its respective eigenvector.

The controllability Gramian is assumed to be positive-definite throughout the optimization process. However, an eigenvalue close to zero indicates that a state might be in a critical condition, i.e., close to be uncontrollable. The proposed optimization formulation aims to maximize the controllability by choosing the best distribution of piezoelectric material (actuators) and ensure that the system will be completely controllable. Thus, the optimization problem can be written as

$$\max \lambda_1 \tag{21}$$

subject to

$$V = \frac{\int_{\Omega} \rho d\Omega}{\int_{\Omega} d\Omega} \leq V^{\max} \quad (22)$$

$$0 \leq \rho_i \leq 1 \quad (23)$$

where λ_1 is the smallest eigenvalue of \mathbf{W}_c . This formulation takes into account the possibility of repeated eigenvalues (Wu *et al.* 2007) of the controllability Gramian. However, it is restricted to consider distinct eigenvalues for the modal problem.

4.2 Sensitivity analysis

The search for the optimal set of design variables uses an SLP algorithm. As a first order method, it requires the sensitivities of the objective function and constraints with respect to design variables. The sensitivity of the controllability Gramian can be obtained by solving a new Lyapunov equation for $\partial \mathbf{W}_c / \partial \rho_i$

$$\mathbf{A} \frac{\partial \mathbf{W}_c}{\partial \rho_i} + \frac{\partial \mathbf{W}_c}{\partial \rho_i} \mathbf{A}^T + \frac{\partial \mathbf{A}}{\partial \rho_i} \mathbf{W}_c + \mathbf{W}_c \frac{\partial \mathbf{A}^T}{\partial \rho_i} + \frac{\partial \mathbf{B}}{\partial \rho_i} \mathbf{B}^T + \mathbf{B} \frac{\partial \mathbf{B}^T}{\partial \rho_i} = \mathbf{0} \quad (24)$$

In order to solve this equation, the sensitivities of the state-space parameters \mathbf{A} and \mathbf{B} with respect to design variables are required. These terms are straightforward and can be obtained by the derivatives of Eqs. (13) with respect to ρ_i . More details on these sensitivities can be found in Silveira *et al.* (2015).

Considering the problem presented in Eqs. (19)-(20), eigenvalue derivatives with respect to ρ_i can be obtained by solving a new eigenanalysis problem (Wu *et al.* 2007)

$$\left[\boldsymbol{\sigma}_j^T \left(\frac{\partial \mathbf{W}_c}{\partial \rho_i} \right) \boldsymbol{\sigma}_j - \frac{\partial \lambda_j}{\partial \rho_i} \right] \gamma_j = \mathbf{0} \quad (25)$$

The derivatives of the coupled finite element model with respect to the design variables are required to find the sensitivities of the state-space parameters \mathbf{A} and \mathbf{B} . The sensitivity of the global piezoelectric coupling matrix is obtained from the superposition of the elemental piezoelectric coupling matrices

$$\frac{\partial \mathbf{K}_{u\phi}^e}{\partial \rho_i} = \int_{\Omega^e} \mathbf{B}_u^T \frac{\partial \mathbf{E}^T}{\partial \rho_i} \mathbf{B}_\phi d\Omega \quad (26)$$

where \mathbf{B}_u is the matrix that relates mechanical strain with displacement and \mathbf{B}_ϕ is the matrix that relates electric field with electric potential. The material parametrization, Eqs. (1)-(4), depends on the design variables ρ_i and therefore its sensitivity can be easily obtained. Likewise, other derivatives such as mechanical stiffness and mass matrices can be derived.

5. Numerical results

5.1 Example structure and analyzed cases

This section presents results for a example structure, a cantilever beam with rectangular cross section shown in Fig. 2, measuring 600 mm× 150 mm× 20 mm (length, height, and width). The beam was discretized using 4800 8-node nonconforming (Taylor *et al.* 1976) brick finite elements presenting three mechanical and one electrical degrees of freedom per node. In this study, only in-plane (xy) vibration modes are considered and controlled.

The constitutive properties of the isotropic elastic material and the piezoelectric material are shown in Tables 1 and 2. The piezoelectric ceramic is polarized in z-direction and thus uses the 31 mode.

Table 1 Piezoelectric material properties (PZT-5A)*

elastic constants	(10 ¹⁰ N/m ²)
C ₁₁	12.1
C ₁₂	7.54
C ₁₃	7.52
C ₃₃	11.1
piezoelectric constants	(C/m ²)
E ₃₁	-5.4
E ₃₃	15.8
E ₅₁	12.3
dielectric constants	(F/m)
ε ₀	8.85·10 ¹²
ε ₁₁ /ε ₀	916
ε ₃₃ /ε ₀	830
density	(kg/m ³)
γ _{pzt}	7750

* Rubio *et al.* (2009)

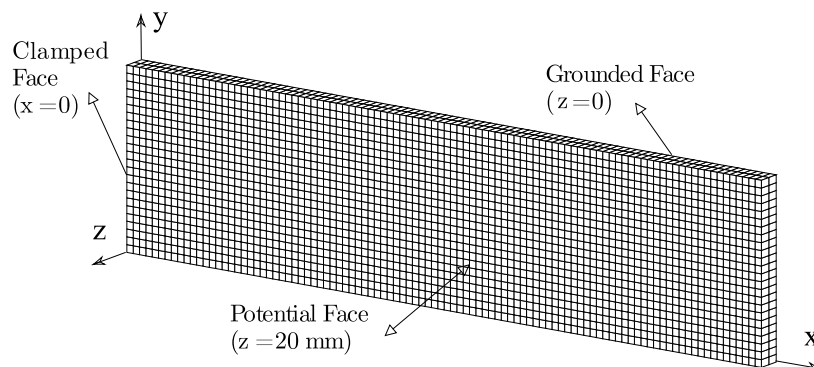


Fig. 2 Finite element model (4800 brick elements) and faces configuration

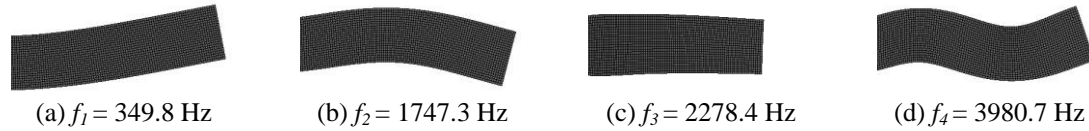


Fig. 3 Vibration modes considered in the control system.

Table 2 Elastic material properties (Aluminum)

Young's modulus	$71 \cdot 10^9 \text{ N/m}^2$
density	2700 kg/m^3
Poisson's ratio	0.33

Vibration modes with the four lower frequencies were assumed as the most representative for the dynamic response of the structure. For this particular structure, the natural vibration modes which are considered are: the first and second bending modes, the first extension mode, and the third bending mode, which have well-spaced natural frequencies. The modal shapes of these vibration modes are presented in Fig. 3 with their respective natural frequencies.

For the dynamic analysis, modal damping ratios of 1.71%, 0.72%, 0.42% and 0.41% (Vasques and Rodrigues 2006) were considered for these four modes. For the controllability analysis, the number of modes m used to build the reduced model can assume values 1, 2, or 4. Considering that geometry does not change, both materials have similar stiffnesses, and the piezoelectric volume constraint is very small, there is no significant change on natural frequencies and modes during the optimization process. Thus, this example avoids the problem of repeated eigenvalues, which requires non-smooth sensitivity analysis and optimization methods (Seyranian *et al.* 1994).

The number and position of independent electrodes are predefined. Cases with one, two and six independent electrodes were analyzed, i.e., number of control inputs s can assume values 1, 2, or 6. These different potential face configurations are represented in Fig. 4. In this figure, the gray areas represent the independent electrodes. The electrical degrees of freedom were ignored in the remaining (white) areas to enable the electrodes independence.

Nine cases were studied according to the number of control inputs and modes used to build the reduced model. The description of these cases are summarized in Table 3.

Sequential linear programming (SLP) was used to solve the optimization problem. SLP is an iterative algorithm, in which the non-linear problem is solved as a sequence of linear programming problems.

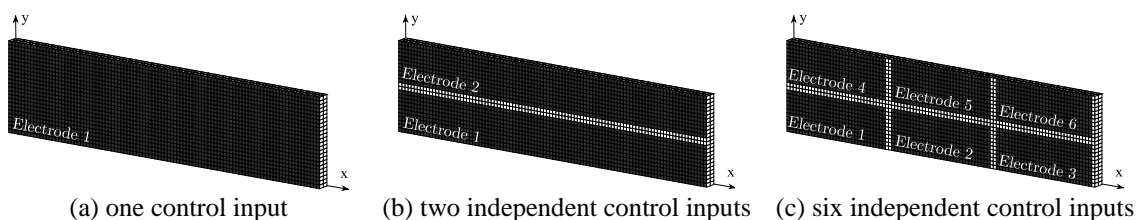


Fig. 4 Potential face configurations

Table 3 Description of the analyzed cases

Case No.	Number of controlled modes (m)	Number of control inputs (s)
1	1	1
2	1	2
3	1	6
4	2	1
5	2	2
6	2	6
7	4	1
8	4	2
9	4	6

For the optimization process, the piezoelectric volume constraint was chosen as 8% for the piezoelectric volume constraint and a cubic penalization was used for both penalty exponents. The starting point for all cases was a uniform distribution of the design variable just obeying the constraint. The convergence criteria was defined as less than 2% maximum change of objective function and less than 4% maximum change of design variables, from one iteration to another. As the optimization problem is non-convex, the gradient-based programming guarantees only local minima.

The weighting matrices of the LQR regulator are the same for every test case and given by (Silveira *et al.* 2015)

$$\mathbf{Q} = \begin{bmatrix} 1 \cdot 10^{17} \mathbf{I}(m) & 0 \\ 0 & \mathbf{I}(m) \end{bmatrix} \quad \mathbf{R} = \mathbf{I}(s) \quad (27)$$

where $\mathbf{I}(m)$ is the m -dimensional identity matrix, and $\mathbf{I}(s)$ is the s -dimensional identity matrix. The large values of matrix \mathbf{Q} components are explained by the difference in magnitude between displacements and voltages. However, these weighting matrices could have been tuned to achieve better response times and to respect the piezoelectric material polarization limit voltages or mechanical stresses.

5.2 Optimal piezoelectric material distribution

Optimal distribution of active piezoelectric material was obtained for the electrodes sets presented in Fig. 4. Reduced models with one, two, and four modes of vibration were considered. Both proposed and Silveira *et al.* (2015) formulations were implemented in order to compare their influence on the system controllability. In this section, white elements represent the elastic isotropic material and black elements represent the piezoelectric material.

Fig. 5 presents the optimal topologies for the cases which consider only the first vibration mode. Cases 1, 2, and 3 refer to the different predefined configurations: one, two, and six independent electrodes.

When only the first mode is considered in the control system, the proposed formulation leads to

piezoelectric material distributions which are similar to the optimal designs obtained in (Silveira *et al.* 2015). In case 1, with only one electrode in the whole structure, the piezoelectric material was concentrated near the bottom left corner. There is no significant difference between cases 2 and 3, with two and six independent electrodes, respectively. In these cases, the active material was concentrated near both upper and bottom left corners. Thus, it is possible to cause simultaneously both tensile and compressive strains providing a more effective vibration control.

In Fig. 6, optimal topologies are presented for cases considering two vibration modes in the control system. For case 4, the proposed formulation seems to favor the second vibration mode since there is no piezoelectric distribution on the clamped face. Cases 5 and 6 present different actuator shapes although the effective electrodes are the same for both formulations.

Cases 7, 8, and 9 are presented in Fig. 7, which shows the optimal topologies obtained considering four vibration modes. For these cases, the choice of objective function caused a significantly different distribution of active material.

Solutions obtained through topology optimization with material interpolation often require post processing to interpret the optimal design. In these studied cases, this interpretation is relatively straightforward since there are few design variables with intermediate values (gray elements). Smoother optimal designs could have been achieved by using density or sensitivity filters (Sigmund 1997) but it would incur in a higher computational cost.

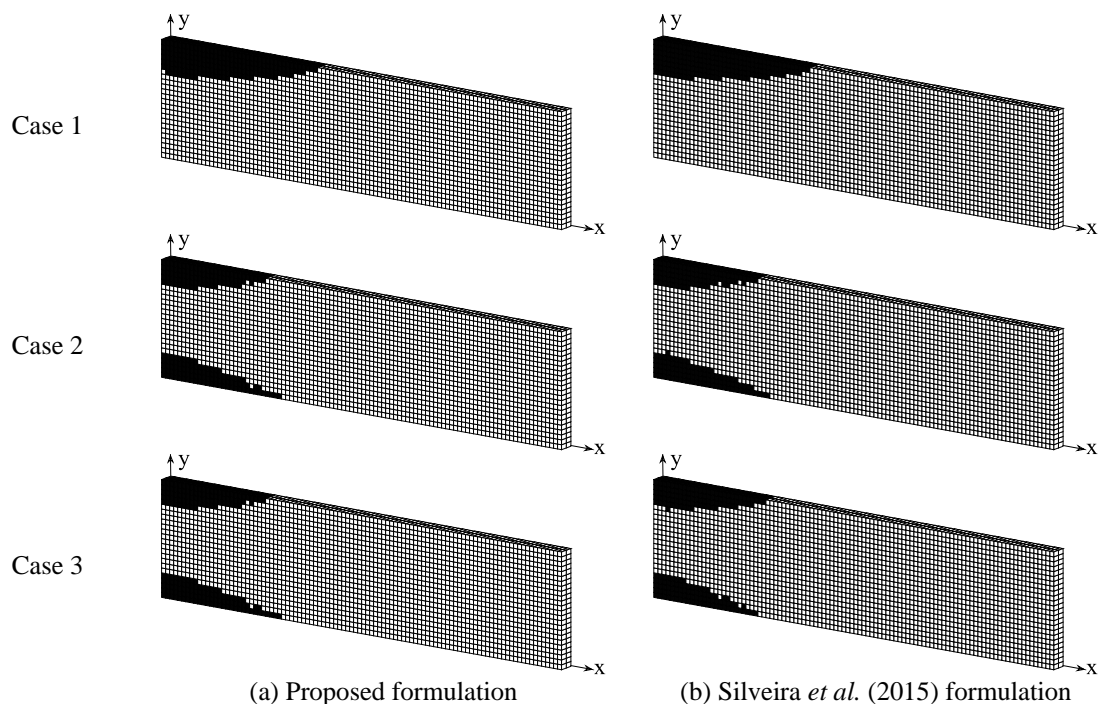


Fig. 5 Optimal piezoelectric material distribution for 1-mode control cases

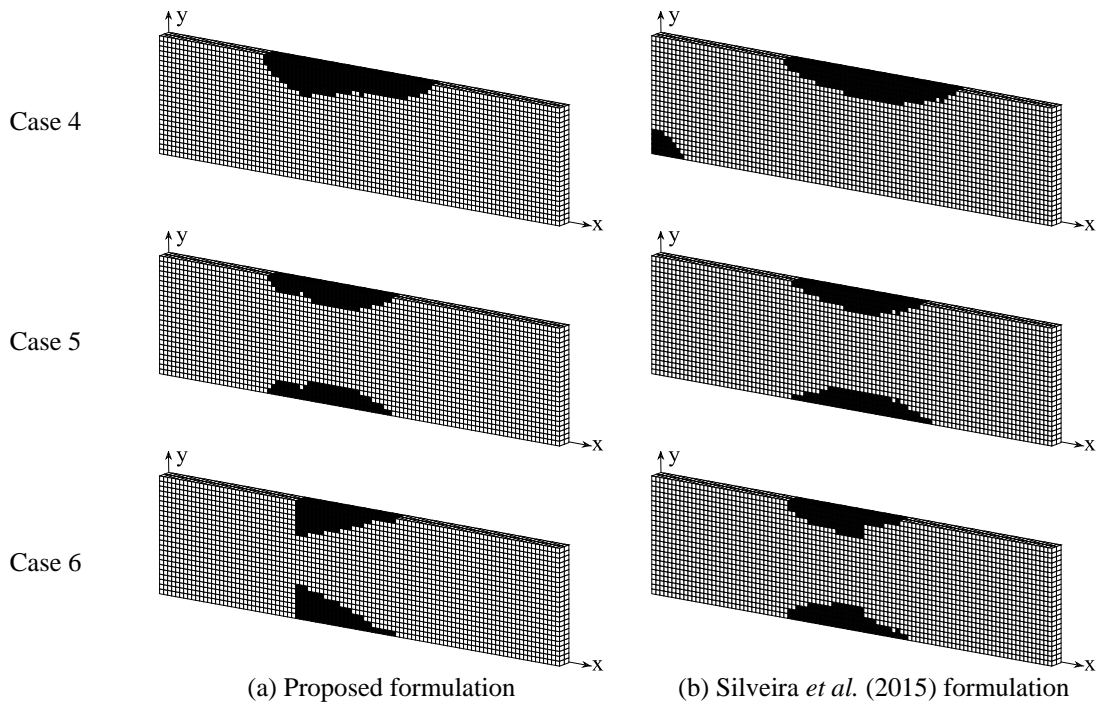


Fig. 6 Optimal piezoelectric material distribution for 2-mode control cases

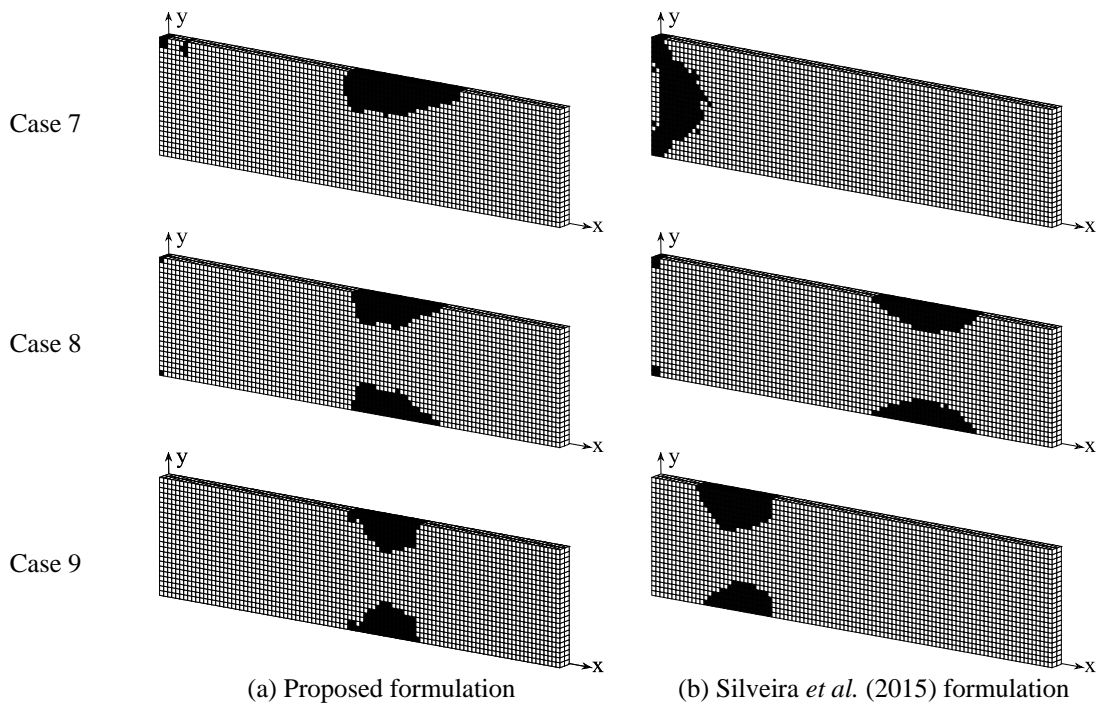


Fig. 7 Optimal piezoelectric material distribution for 4-mode control cases

5.3 Convergence of objective functions

Changes in the values of objective functions throughout the iterations history are discussed in this section. Both controllability measures (CM) are presented in order to observe how is their behavior during the optimization process. For a better visualization, the objective function is represented by a solid line with circular markers while the other CM is represented by a dashed line with cross-shaped markers. The convergence history for case 5 is presented in Fig. 8 where can be observed that a maximization of a CM also caused an increase in the value of the other.

The proposed formulation presented a slow and irregular λ_1 convergence for case 7, as shown in Fig. 9. However, this maximization caused a significant increase in other CM. The converged CM values may indicate that the solution (b) is a local maximum of the problem.

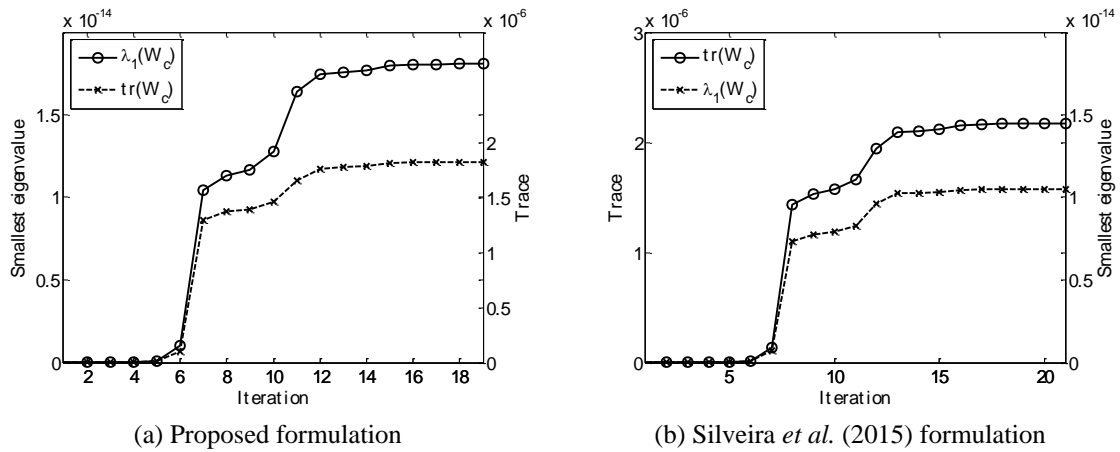


Fig. 8 CM history for case 5

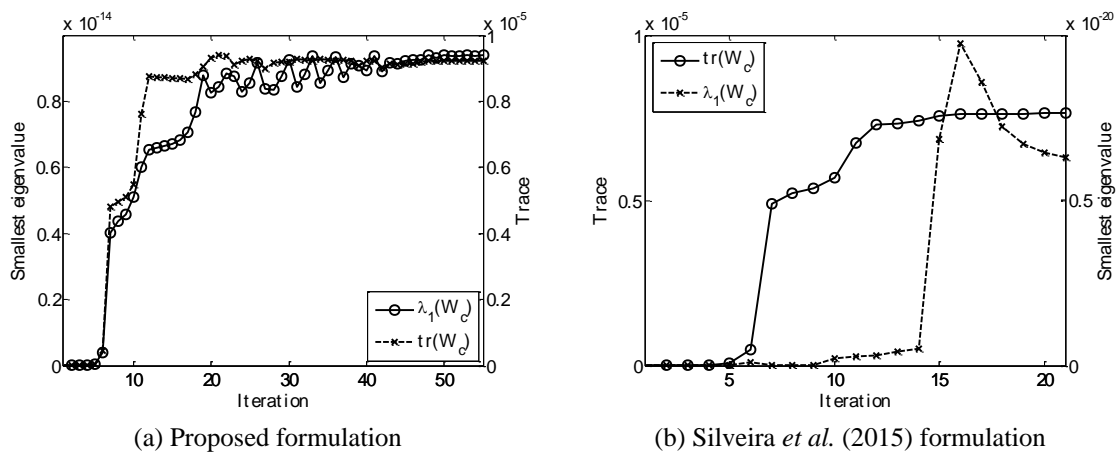


Fig. 9 CM history for case 7

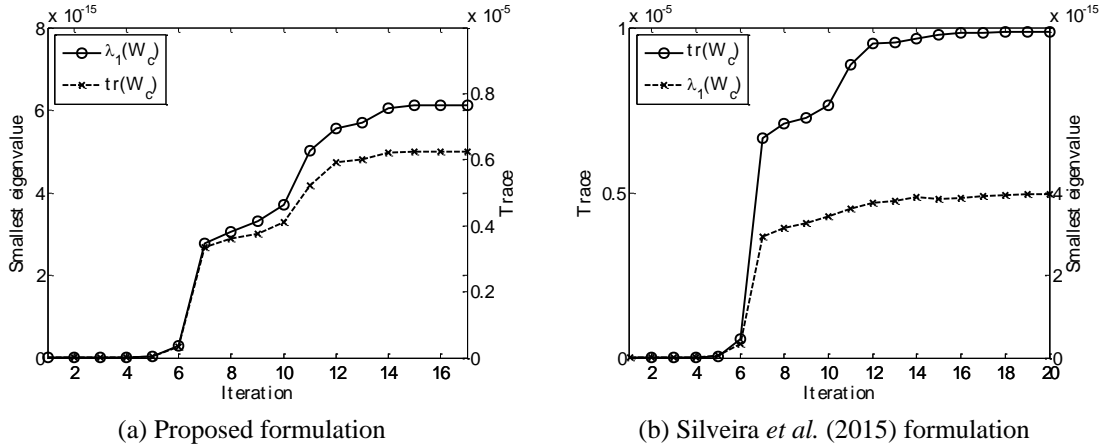


Fig. 10 CM history for case 8

Fig. 10 exposes the convergence history for case 8. Unlike the previous case, the convergence curves present regular behavior and the maximum values of each CM are consistent with the maximization that was performed.

5.4 Unit impulse response of a dynamic system

Responses to an impulsive load on the free-end of the cantilever beam were obtained and are presented in this section. This study considers a discrete-time system and, consequently, the dynamic response is obtained with respect to a unit area input pulse lasting T_s (sampling time) assuming null values to the initial states. Although finite element method was used to evaluate the natural frequencies and its vibration modes to create the control models in state-space representation, it was not directly used in transient analysis.

Figs. 11-16 show the responses in terms of the vertical displacement at the free-end of the beam and input signals. The displacements for the controlled structure in open-loop and closed-loop are represented by solid and dotted lines, respectively. To compare the performance of controlled structures (CS), two parameters are considered: maximum vertical displacement (U_m) and the RMS value of vertical displacement (U_{rms}), both measured on the free-end of the beam. The comparison between open-loop and closed-loop response is presented separately for each structure since the distribution of piezoelectric material can modify its dynamic characteristics. Relative reductions RU_i for both maximum and RMS measures were also used for comparison analysis and they are defined as

$$RU_i = \frac{|U_i^{OL} - U_i^{CL}|}{U_i^{OL}} 100\% \quad (28)$$

where the subscript i can refer to maximum m or rms measure and the superscripts OL and CL relates to the open-loop and closed loop responses, respectively.

Fig. 11 presents the responses for case 5. In this case, for the CS (a) there is a reduction in U_m of 15.5% while for the CS (b) the reduction is 12.0%. Considering the parameter U_{rms} , for the CS

(a) it is observed a reduction of 63.7% while for the CS (b) the reduction is 57.7%. Fig. 12 presents the respective input signals for this case.

Responses for case 8 are presented in Fig. 13. For the CS (a) there is a reduction in U_m of 10.2% while for the CS (b) the reduction is 7.4 %. Considering the parameter U_{rms} , for the CS (a) it is observed a reduction of 52.0% while for the CS (b) the reduction is 47.1%. Fig. 14 presents the respective input signals for this case.

Fig. 15 presents the responses for case 9. In this case, for the CS (a) there is a reduction in U_m of 8.5% while for the CS (b) the reduction is 18.7%. Considering the parameter U_{rms} , for the CS (a) it is observed a reduction of 47.4% while for the CS (b) the reduction is 69.1%. Fig. 16 presents the respective input signals for this case. Fig. 17 presents the free tip displacement percentage reduction for all analyzed cases. The proposed formulation presents better performance for cases with less control inputs, which is the opposite trend of the formulation proposed by Silveira *et al.* (2015).

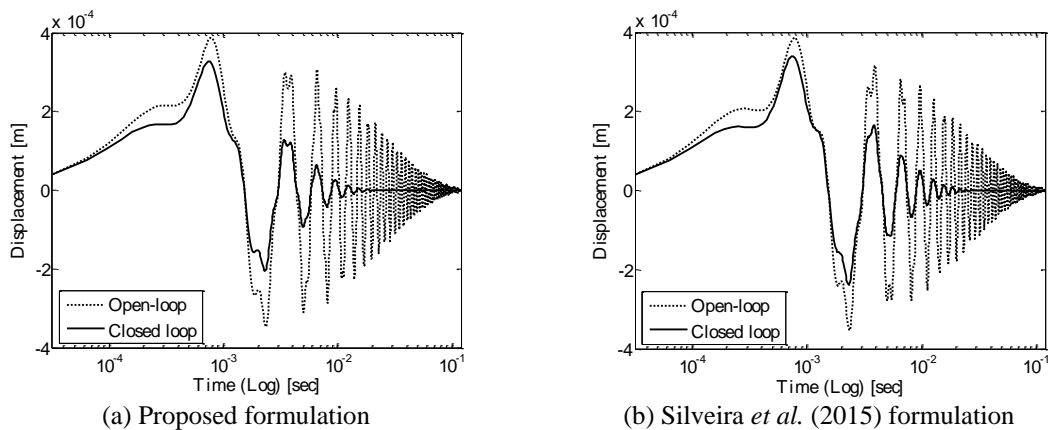


Fig. 11 Free tip displacement response to an impulsive load for case 5

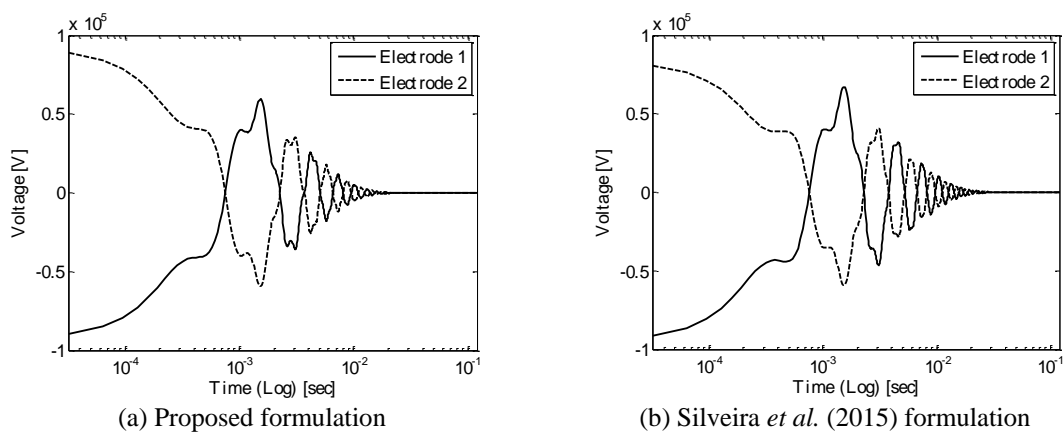


Fig. 12 Control signal for case 5

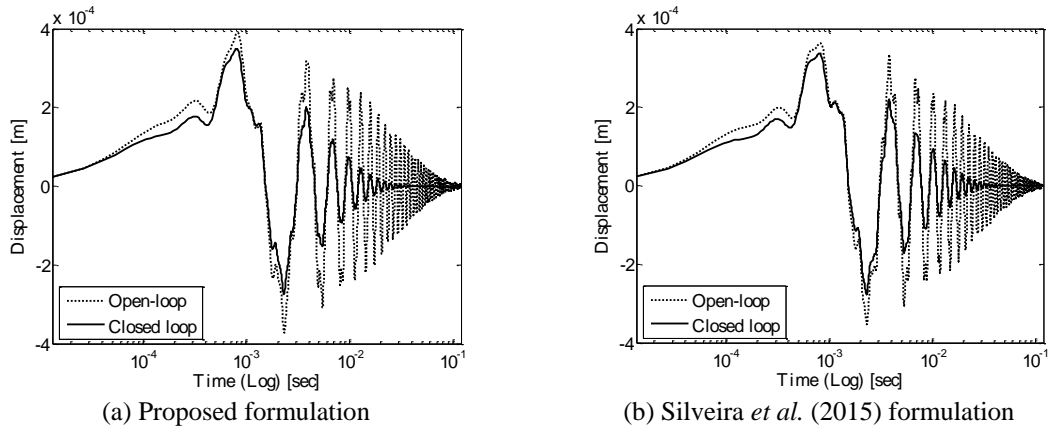


Fig. 13 Free tip displacement response to an impulsive load for case 8

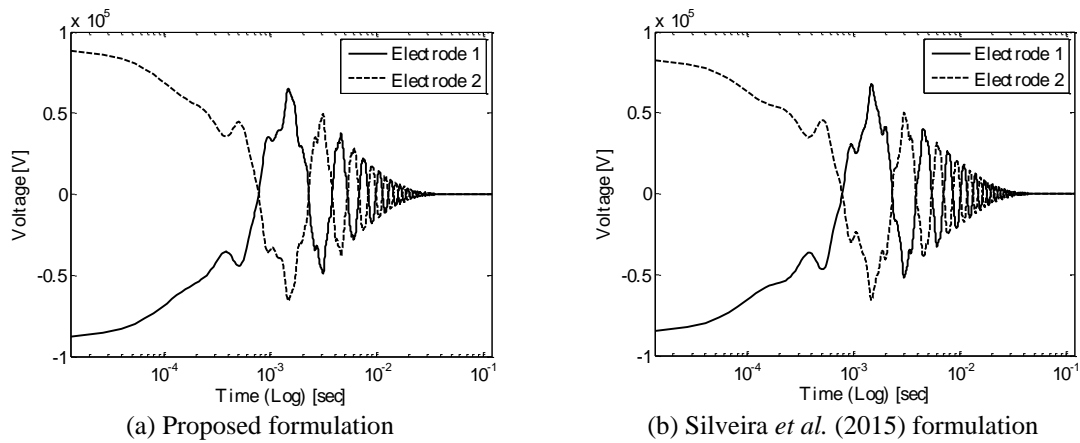


Fig. 14 Control signal for case 8

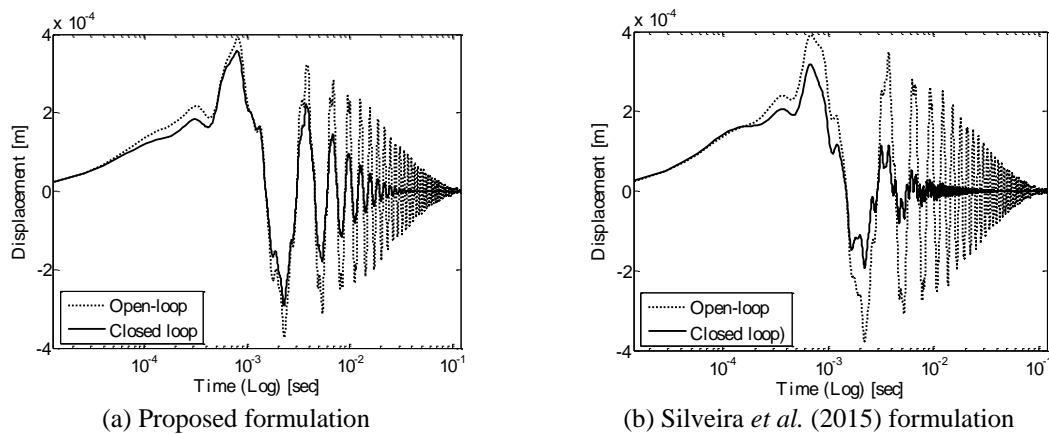


Fig. 15 Free tip displacement response to an impulsive load for case 9

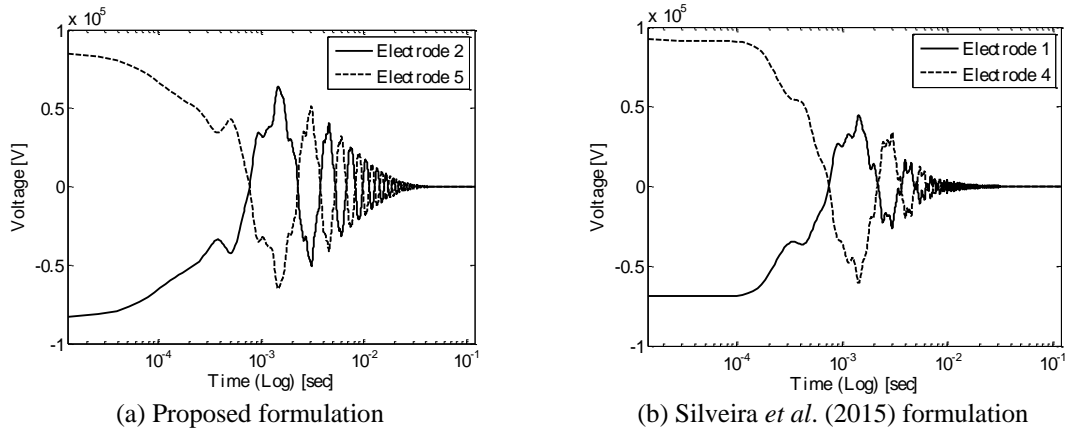


Fig. 16 Control signal for case 9

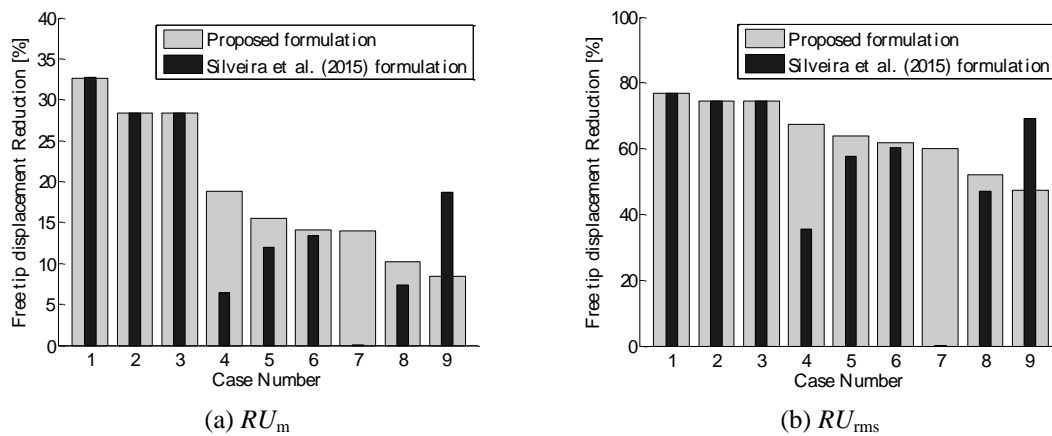


Fig. 17 Comparison parameters reduction

Moreover, case 9 was the only one where the proposed formulation presents significantly smaller reductions for both U_m and U_{rms} . It can be explained by the fact that the proposed formulation gives more importance to higher vibration modes (less controllable for this particular example) while Silveira *et al.* (2015) formulation gives more importance to lower modes, which are the most representative to the global dynamic response. One can note this by analyzing the topologies in Fig. 7 where the solution for the proposed formulation presents active material close to points with maximum displacement of the fourth vibration mode.

6. Conclusions

This work presents a formulation based on the controllability Gramian for the optimal placement of piezoelectric actuators for structural vibration control. The proposed formulation aims to maximize the control effectiveness and ensure the controllability of every state, which can

be ensured by using the smallest eigenvalue of \mathbf{W}_c as the objective function to be maximized.

Optimal topologies were presented for some cases where the number and location of the independent electrodes are predefined. These solutions were compared to the ones obtained through the formulation proposed by Silveira *et al.* (2015), where the trace of \mathbf{W}_c is maximized. Using either the smallest eigenvalue or the trace of the Gramian as objective function, the optimization process leads to the same solution when only the first mode is considered to be controlled. This is explained by the choice of state variable vector which has dependent terms (modal displacement and velocity). There is a more significant difference regarding the choice of controllability measure to be maximized when more than one mode is considered in the control system.

The optimal designs were used to synthesize a feedback control system using a linear quadratic regulator (LQR) in order to compare their control performance. Dynamic responses to an impulsive perturbation were presented for both formulations. Using Silveira *et al.* (2015) formulation it is improved the controllability of the most controllable states. On the other hand, following the proposed formulation leads to an improvement on the controllability of the less controllable mode. This condition guarantee that there will be none state in a critical situation, i.e., close to be uncontrollable. For the most analyzed cases it was observed that a maximization of one controllability measure contributes for an increase on the other, resulting thus in controllable systems regardless the choice of objective function. As expected, cases with control system considering four vibration modes presented difficulties to attenuate vibrations due to the compromise that is induced, i.e., the control system need to be effective at the same time for all modes. Individual electrodes to control each vibration mode could improve the global controllability for these cases. Therefore, the proposed formulation would fit better since each modal controllability can be directly related to a single eigenvalue of \mathbf{W}_c .

Acknowledgments

The authors acknowledge the financial support of the Brazilian agencies CNPq and CAPES.

References

- Allik, H. and Hughes, T.J.R. (1995), "Finite element method for piezoelectric vibration", *Int. J. Numer. Meth. Eng.*, **2**, 151-157.
- Balas, M.J. (1978), "Feedback control of flexible systems", *IEEE T. Automat. Contr.*, **23**(4), 673-679.
- Bartels, R.H. and Stewart, G.W. (1972), "Solution of the matrix equation $ax + xb = c$ [f4]", *Commun. ACM*, **15**(9), 820-826.
- Bendsøe, M.P. (1989), "Optimal shape design as a material distribution problem", *Struct. Optimization*, **1**, 193-202.
- Bendsøe, M.P. and Sigmund, O. (1999), "Material interpolation schemes in topology optimization", *Arch. Appl. Mech.*, **69**, 635-654.
- Bendsøe, M.P. and Kikuchi, N. (1988), "Generating optimal topologies in structural design using a homogenization method", *Comput. Method. Appl. M.*, **71**(2), 197-224.
- Burl, J.B. (1999), *Linear Optimal Control*, Addison-Wesley, California, USA.
- Gawronski, W. (2004), *Advanced Structural Dynamics and Active Control of Structures*, Springer-Verlag, New York, USA.

- Gawronski, W. and Lim, K.B. (1996), "Balanced actuator and sensor placement for flexible structures", *Int. J. Control.*, **65**, 131-145.
- Gupta, V., Sharma, M., Thakur, N. and Singh, S.P. (2011), "Active vibration control of a smart plate using a piezoelectric sensor-actuator pair at elevated temperatures", *Smart Mater. Struct.*, **20**(10), 105023.
- Hać, A. and Liu, L. (1993), "Sensor and actuator location in motion control of flexible structures", *J. Sound Vib.*, **167**(2), 239-261.
- Hamdan, A.M.A. and Nayfeh, A.H. (1989), "Measures of modal controllability and observability for first and second-order linear systems", *J. Guid. Control. Dynam.*, **12**(3), 421-428.
- Kim, J.E., Kim, D.S., Ma, P.S. and Kim, Y.Y. (2010) "Multi-physics interpolation for the topology optimization of piezoelectric systems", *Comput. Method. Appl. M.*, **199**(49), 3153-3168.
- Kim, Y. and Junkins, J.L. (1991), "Measure of controllability for actuator placement", *J. Guid. Control. Dynam.*, **14**, 895-902.
- Kumar, K.R. and Narayanan, S. (2008), "Active vibration control of beams with optimal placement of piezoelectric sensor/actuator pairs", *Smart Mater. Struct.*, **17**(5), 055008.
- Leleu, S., Abou-Kandil, H. and Bonnassieux, Y. (2001), "Piezoelectric actuators and sensors location for active control of flexible structures", *IEEE T. Instrum. Meas.*, **50**(6), 1577-1582.
- Meirovitch, L. (1990), *Dynamics and Control of Structures*, John Wiley & Sons, New York, USA.
- Onoda, J. and Haftka, R.T. (1987), "An approach to structure/control simultaneous optimization for large flexible spacecraft", *AIAA J.*, **25**(8), 1133-1138.
- Ou, J.S. and Kikuchi, N. (1996), "Integrated optimal structural and vibration control design", *Struct. Optimization*, **12**(4), 209-216.
- Preumont, A. (2002), *Vibration Control of Active Structures, An Introduction*, Kluwer Academic Publisher, Dordrecht, The Netherlands.
- Rubio, W.M., Silva, E.C.N. and Paulino, G.H. (2009), "Toward optimal design of piezoelectric transducers based on multifunctional and smoothly graded hybrid material systems", *J. Intel. Mat. Syst. Str.*, **20**(14), 1725-1746.
- Ruiz, D., Bellido, J.C., Donoso, A. and Sánchez-Rojas, J.L. (2013), "Design of in-plane piezoelectric sensors for static response by simultaneously optimizing the host structure and the electrode profile", *Struct. Multidiscip. O.*, **48**(5), 1023-1026.
- Seyranian, A.P., Lund, E. and Olhoff, N. (1994), "Multiple eigenvalues in structural optimization problems", *Struct. Optimization*, **8**(4), 207-227.
- Sigmund, O. (1997), "On the design of compliant mechanisms using topology optimization", *Mech. Struct. Machines*, **25**(4), 493-524.
- Sigmund, O. and Petersson, J. (1998), "Numerical instabilities in topology optimization: A survey on procedures dealing with checkerboards, mesh-dependencies and local-minima", *Struct. Optimization*, **16**(1), 68-75.
- Silva, E.C.N. and Kikuchi, N. (1999), "Design of piezoelectric transducers using topology optimization", *Smart Mater. Struct.*, **8**(3), 350.
- Silveira, O.A.A., Fonseca, J.S.O. and Santos, I.F. (2015), "Actuator topology design using the controllability gramian", *Struct. Multidiscip. O.*, **51**(1), 145-157.
- Sohn, J.W., Choi, S. and Kim, H.S. (2011), "Vibration control of smart hull structure with optimally placed piezoelectric composite actuators", *Int. J. Mech. Sci.*, **53**(8), 647-659.
- Takezawa, A., Kitamura, M., Vatanabe, S.L. and Silva, E.C.N. (2014), "Design methodology of piezoelectric energy-harvesting skin using topology optimization", *Struct. Multidiscip. O.*, **49**(2), 281-297.
- Takezawa, A., Makiyama, K., Kogiso, N. and Kitamura, M. (2014), "Layout optimization methodology of piezoelectric transducers in energy-recycling semi-active vibration control systems". *J. Sound Vib.*, **333**(2), 327-344.
- Takezawa, A., Nishiwaki, S., Kitamura, M. and Silva, E.C.N. (2010), "Topology optimization for designing strain-gauge load cells", *Struct. Multidiscip. O.*, **42** (3), 387-402.
- Taylor, R.L., Beresford, P.J. and Wilson, E.L. (1976), "A non-conforming element for stress analysis", *Int. J. Numer. Methods in Engineering*, **10**(6), 1211-1219.

- Vasques, C.M.A. and Rodrigues, J.D. (2006), "Active vibration control of smart piezoelectric beams: Comparasion of classical and optimal feedback control strategies", *Comput. Struct.*, **84**, 1402-1414.
- Wang, Q. and Wang, C.M. (2001), "A controllability index for optimal design of piezoelectric actuators in vibration control of beam structures", *J. Sound Vib.*, **242**(3), 507-518.
- Wu, B., Xu, Z. and Li, Z. (2007), "A note on computing eigenvector derivatives with distinct and repeated eigenvalues", *Commun. Numer. Meth. En.*, **23**, 241-251.
- Zhang, X. and Kang, Z. (2014), "Dynamic topology optimization of piezoelectric structures with active control for reducing transient response", *Computer Methods in Applied Mechanics and Engineering*, **281**, 200-219.

CC